Supplementary Information for:

"Great reduction of hole effective mass of wide in bandgap semiconductors by highly mismatched alloying"

Sixin Kang,[a] Shuaiwei Fan,*[a b] and Gongwei Hu[a]

[a] Department of Physics, China Three Gorges University, Yichang 443002, China

[b] Hubei Engineering Research Center of Weak Magnetic-field Detection, China Three Gorges University, Yichang 443002, China

1 Stability of alloys

1.1 Elastic constants

To verify the mechanical stability of the $LiGa(Se_{1-x}O_x)_2$ alloys, their elastic constants are calculated and listed in Table S1. There are nine independent constants in the orthorhombic crystal system, which are C_{11}, C_{12}, C_{13}, C_{22}, C_{23}, C_{33}, C_{44}, C_{55}, and C_{66}. For mechanical stability, each of these elastic constants must satisfy the following conditions:[S1,2]

$$C_{ii} > 0 \ (i = 1, 4, 5, or\ 6),$$
$$C_{11}C_{22} > C_{12}^2, \qquad \backslash^*$$
$$C_{11}C_{22}C_{33} + 2C_{12}C_{13}C_{23} - C_{11}C_{23}^2 - C_{22}C_{13}^2 - C_{33}C_{12}^2 > 0.$$

MERGEFORMAT (1)

The calculated elastic constants of the alloys satisfy the stability condition given in Eq. (1), indicating that the alloys are mechanically stable at ambient pressure.

Table S1 The Calculated elastic constants for the orthorhombic $LiGa(Se_{1-x}O_x)_2$ alloys are listed.

Alloy composition / Elastic constants	6.25%	12.50%	18.75%	25.00%
C_{11}	64.894	52.5	70.500	56.363
C_{12}	15.66	5.293	19.45	5.608
C_{13}	13.781	2.686	16.175	6.28
C_{22}	58.521	61.341	67.405	64.375
C_{23}	21.681	19.851	26.612	19.541
C_{33}	43.876	45.124	46.781	52.167
C_{44}	19.283	19.24	21.000	22.838
C_{55}	18.1	17.518	18.043	16.458
C_{66}	14.912	16.471	15.355	16.19

1.2 Phonon spectra

To confirm the semiconductor $LiGa(Se_{1-x}O_x)_2$ alloys' dynamic stability, the phonon dispersion curves and the elemental contributions are calculated using the vaspkit software package[S3] and zoomed in on the states around the zero point, as shown in Fig. S1. The phonon spectra exhibit no imaginary frequencies in the Brillouin zone, indicating that the disordered semiconductor alloys' structure is dynamically stable.

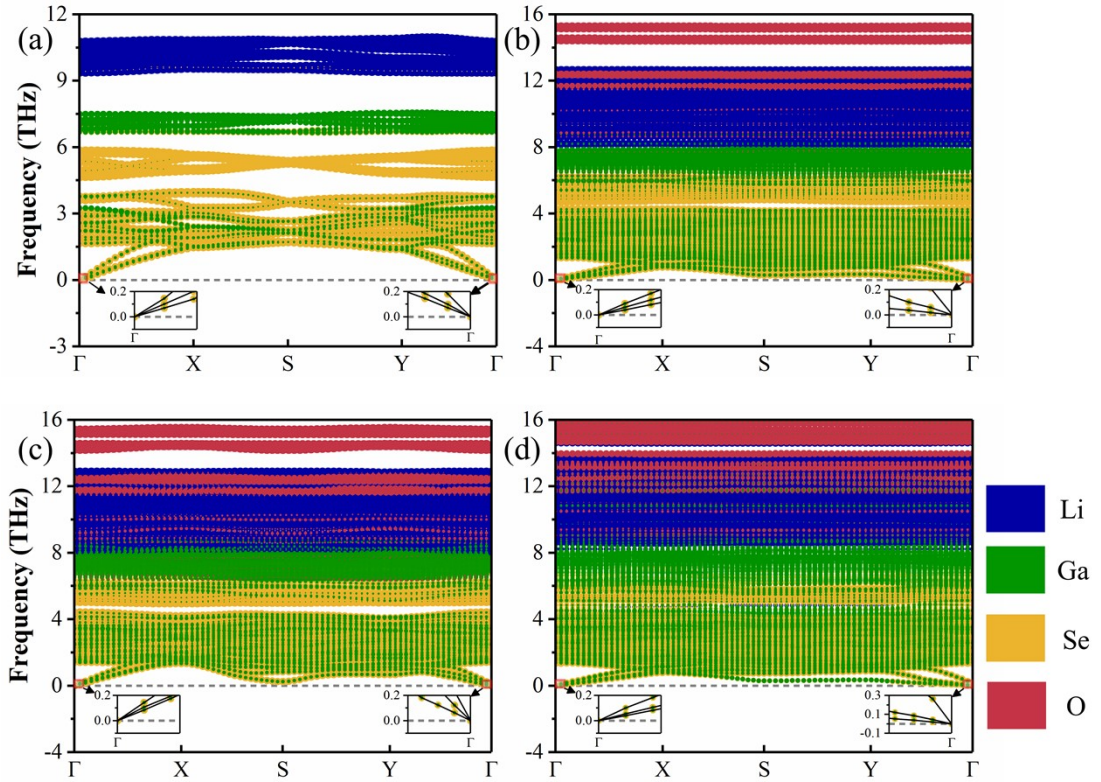

Fig. S1 The phonon dispersion curves of the semiconductor $LiGa(Se_{1-x}O_x)_2$ alloys at (a) 0%, (b) 6.25%, (c) 12.50%, and (d) 25.00% oxygen composition (x) are plotted, where the contributions of Li, Ga, Se, and O atoms are shown in blue, green, yellow, and red, respectively.

2 Density of states

The partial density of states (pDOS) of $LiGaSe_2$ and $LiGa(Se_{0.75}O_{0.25})_2$ alloy is shown in Fig. S2. This figure corresponds to Fig. 5 in the main text, and the same conclusion can be drawn.

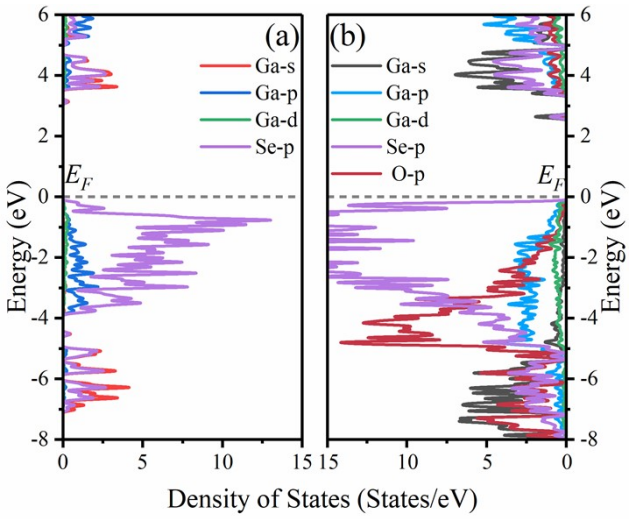

Fig. S2 The PDOS for $LiGaSe_2$ (a) and $LiGa(Se_{0.75}O_{0.25})_2$ alloy (b), calculated using HSE, are illustrated, with the Fermi energy (E_F) set to zero.

3 Crystal structures

The crystal structures of the semiconductor $LiGa(Se_{1-x}O_x)_2$ alloys are shown in Fig. S3, with Li, Ga, Se, and O atoms represented by silver, yellow, green, and red spheres, respectively.

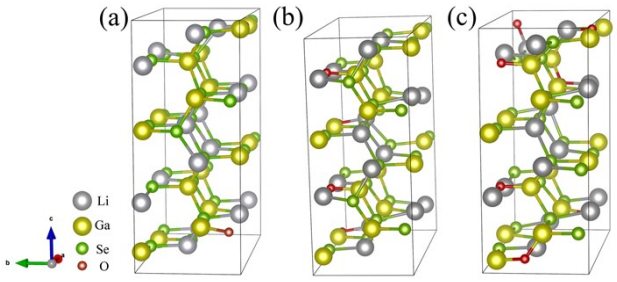

Fig. S3 The crystal structures of semiconductor $LiGa(Se_{1-x}O_x)_2$ alloys at (a) 6.25%, (b) 12.50%, and (c) 25.00% compositions are depicted, with Li, Ga, Se, and O atoms represented by silver, yellow, green, and red spheres, respectively.

4 Carrier effective mass

The effective masses of electrons and holes along the Γ-Y and Γ-Z directions for the $LiGa(Se_{1-x}O_x)_2$ alloys are summarized in Table S2. For the alloys, the effective masses of electrons and holes along the Γ-Y direction are optimal.

Table S2 The calculated effective masses (m_0) of electron (m^* e) and hole (m^* h) along the Γ-Y

direction and Γ-Z direction for $LiGa(Se_{1-x}O_x)_2$ alloys are listed, where the fitting errors are given for each value.

$LiGa(Se_{1-x}O_x)_2$ / m^*		0%($LiGaSe_2$)	x=6.25%	x=12.50%	x=25.00%
m^* e	Γ-Y	0.261(±2.3×10^{-8})	0.327(±7.7×10^{-8})	0.294(±6.7×10^{-9})	0.289(±5.7×10^{-7})
	Γ-Z	0.231(±1.9×10^{-7})	0.372(±9.8×10^{-9})	0.322(±7.4×10^{-9})	0.358(±1.0×10^{-7})
m^* h	Γ-Y	1.351(±4.9×10^{-8})	0.295(±3.5×10^{-8})	0.376(±5.9×10^{-8})	0.666(±1.2×10^{-6})
	Γ-Z	2.421(±3.6×10^{-10})	2.213(±4.1×10^{-7})	1.957(±4.0×10^{-8})	1.175(±6.1×10^{-8})

5 Valence band edge

The highest valence band edges of the semiconductor $LiGa(Se_{1-x}O_x)_2$ alloys with different compositions near the valence band maximums (VBMs) are plotted in Fig. S4, where the VBMs of their band structure are set to zero.

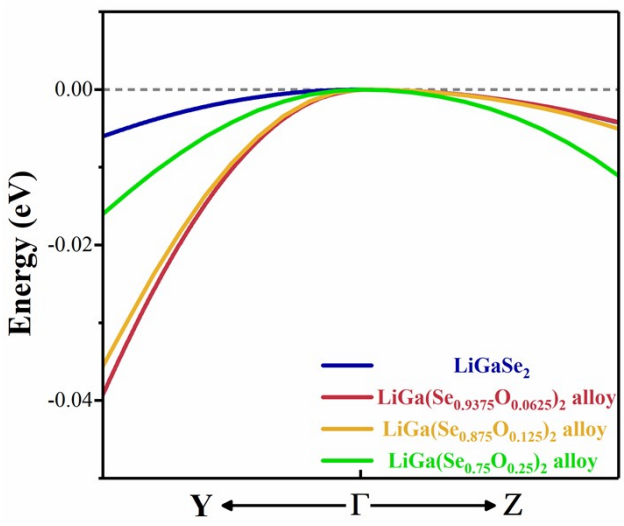

Fig. S4 The highest valence band edge near its maximum in the Y-Γ-Z direction for semiconductor $LiGa(Se_{1-x}O_x)_2$ alloys with different compositions, where the VBMs of their band structure are set to zero.

6 Optical properties of $LiGa(Se_{0.9375}O_{0.0625})_2$ alloy

The calculated real and imaginary parts of the dielectric function for the alloy along each axis are shown in Fig. S5(a). The slight anisotropy in the dielectric function of the alloy along each axis is due to the differences in lattice constants. The transmittance ($T(\omega)$) images along the X, Y, and Z directions in the visible photon energy range for alloys with varying sample thicknesses are depicted in Fig. S5(b)-(d).

The variations in $T(\omega)$ of the alloy along different axes also reflect the slight anisotropy in the dielectric function. This anisotropy does not affect the conclusions presented in this paper.

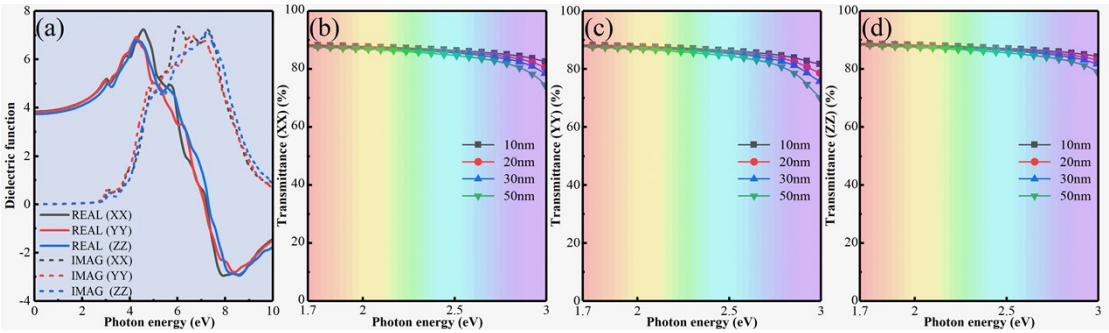

Fig. S5 (a) The real and imaginary parts of the dielectric function for the $LiGa(Se_{0.9375}O_{0.0625})_2$ alloy along different axes are depicted. The optical transmittance of the alloy with varying sample thicknesses in the X, Y, and Z directions as a function of photon energy is shown in (b)-(d).

7 Transport Properties

The carriers' mobility (μ) is calculated using the formula $\mu=e\tau/m^*$ (m^*: carriers' effective mass, and τ: the acoustic phonon scattering relaxation time). Therefore, smaller hole effective mass leads to higher electrical conductivity. In this work, the hole transport properties are calculated using AMSET.[S4] The mobility with carrier concentration at room temperature for $LiGaSe_2$ and $LiGa(Se_{0.9375}O_{0.0625})_2$ alloy is shown in Fig. S6. Both exhibit the same trend in mobility variation, with maximum mobility obtained at low carrier concentration, and decreasing with increasing carrier concentration. The hole mobility of the $LiGa(Se_{0.9375}O_{0.0625})_2$ alloy is higher than that of $LiGaSe_2$ when the hole density increases from 10^{16} to 10^{20} cm^3, which could be attributed to the significant reduction in the hole effective mass of the alloy.[S5]

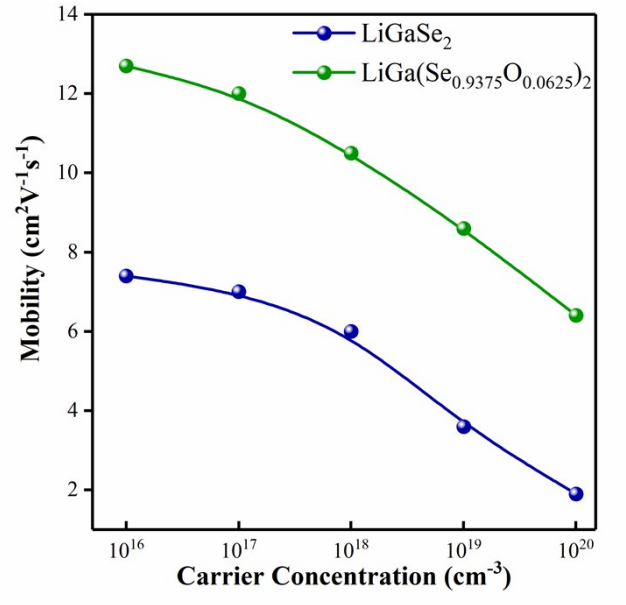

Fig. S6 The calculated hole mobility of $LiGaSe_2$ and $LiGa(Se_{0.9375}O_{0.0625})_2$ alloy over a range of carrier concentrations at room temperature.

References

S1 S. X. Kang, J. Y. Wang and S. W. Fan, *J. Appl. Phys.*, 2024, **136**, 75102.

S2 F. Mouhat and F. Coudert, *Phys. Rev. B*, 2014, **90**, 224104.

S3 V. Wang, N. Xu, J. Liu, G. Tang and W. Geng, *Comput. Phys. Commun.*, 2021, **267**, 108033.

S4 A. M. Ganose, J. Park, A. Faghaninia, R. Woods-Robinson, K. A. Persson and A. Jain, *Nat. Commun.*, 2021, **12**, 2222.

S5 Y. Zhang, K. Yang and H. Deng, *Chin. Phys. Lett.*, 2018, **35**, 56401.